Journal of Sensor Technology, 2024, 14, 68-82
https://www.scirp.org/journal/jst
ISSN Online: 2161-1238
ISSN Print: 2161-122X

Enhanced Meander Antenna for Biomedical Implant Applications

Pacôme Brou[1*], Alex Akohoule[1], Dozohoua Silue[1], Olivier Asseu[1,2]

[1]Laboratoire of LASTIC, Ecole Supérieure Africaine des Technologies de l'Information et de la Communication (ESATIC), Abidjan, Côte d'Ivoire
[2]UMRI STI, Institut National Polytechnique Houphouët BOIGNY (INP-HB), Yamoussoukro, Côte d'Ivoire
Email: *pacome.brou@esatic.edu.ci

How to cite this paper: Brou, P., Akohoule, A., Silue, D. and Asseu, O. (2024) Enhanced Meander Antenna for Biomedical Implant Applications. *Journal of Sensor Technology*, **14**, 68-82.
https://doi.org/10.4236/jst.2024.144005

Received: October 28, 2024
Accepted: December 3, 2024
Published: December 6, 2024

Abstract

In this paper, a design of a miniature antenna for biomedical implant applications is presented. The proposed structure consists of a printed antenna designed to cover all frequency bands below 1 GHz and is dedicated to biomedical applications with good matching, omnidirectional radiation, and a maximum realized gain of −26.7 dBi. It offers two bandwidths of 270 MHz and 762 MHz respectively. A Phantom model of the elliptical cylinder of 180 × 100 × 50 mm^3 was used to simulate the electromagnetic radiation inside the human body. The tissue considered is equivalent to a muscle with a relative permittivity of 57 and a conductivity equal to 0.79 S/m. We also studied the antenna behavior when close to the internal electronic components. The simulation showed that the antenna remains robust in such an environment. Finally, the Specific Absorption Rate of the muscle was evaluated when the antenna was fed with 1 V. The evaluation proved that the calculated value of 0.48 W/Kg is well below the limit value imposed by the International Commission on Non-Ionizing Radiation Protection.

Keywords

Implantable And Miniaturized Antenna, Arcs Curved Antenna, Specific Absorption Rate, Internal Electronic Components, Biomedical Implants

1. Introduction

The increase in the connectivity capacity of new generation networks (NGN) over the last two decades has driven a dynamic in the use of new Information and Communication Technologies (ICT) in the healthcare sector worldwide. According to the Joint Observatory of Computing, Engineering, Studies and Consulting (OPIIEC)

[1], this dynamic not only contributes to patient care, but also facilitates access to information for various professionals and patients. The OPIIEC believes that the use of ICT in medical care facilitates cooperation between professionals and increases the quality of care. Biomedical telemetry is one of the applications of ICT in healthcare. It represents a huge potential to improve the quality of medical care as it allows cooperation, remote intervention of actors and especially the collection of parameters of several pathologies at the same time. However, the major challenge of biomedical telemetry remains the reliability and stability of radio connectivity in or near the human body. Therefore, to meet this challenge, sensor nodes for biomedical telemetry must have antennas that are suitable for the environment characterized by high permittivity. In the paper [2], the authors classified biomedical telemetry antennas into three categories based on their location in or on the body: ingestible antennas (endoscopic capsules), body-mounted antennas (wearable antennas) and implantable antennas.

Whether endoscopic, wearable or implanted, biomedical telemetry antennas must be incorporated into tiny equipment and must contribute to providing quality health care or anticipating the onset of certain pathologies. This requires the design of miniature antennas with good performance in terms of matching, radiation, bandwidth and gain. In addition, most of the antennas proposed in the literature have large dimensions that are detrimental to their use in the human body.

In this study, we propose a meander antenna with a very small size ($9.4 \times 4.7 \times 0.0254\ \text{mm}^3$) for use in human body implants. With a volume of $1.122\ \text{mm}^3$, a minimum reflection of −30 dB and two wide bandwidths of 270 MHz and 762 MHz respectively, these characteristics make the antenna a good candidate for implantable systems. It appears to be smaller than all antennas described in the literature.

The remainder of this article is organized as follows: In section II, a literature review of biomedical telemetry antennas is made. This section not only describes previous work, but also invents the categories and requirements of telemetry antennas. Section III of this study presents the structure and performance of the proposed antenna. In section IV we make a study of the miniaturized antenna, and we also compare the performances of miniaturized antenna with those of other antennas described in the literature. Section V provides an assessment of the Specific Absorption Rate (SAR) of the muscle. Finally, in section VI, we give directions for future work and conclude this study.

2. Literature Review

2.1. Antennas for Endoscopic Capsules

An endoscope is a device placed in a body cavity or more generally in the digestive tract and allows the transmission of medical data in image/video format between the body and the outside world. Wireless endoscopes are increasingly used in comparison to wired endoscopes because they offer a certain comfort to the patient during the clinical examination. Since wireless endoscopes are usually ingested, they can explore several cavities of the digestive tract during their passage. This allows them to explore certain cavities such as the small intestine that are inaccessible to wire endoscopes. According to [3], an endoscopic capsule includes an optical dome, a camera, one or more LEDs, a radio frequency transmitter, an antenna and a battery. The antennas of the endoscopes must be efficient (broadband, good adaptation) to allow the visualization of High Definition (HD) images or videos and the early diagnosis of certain diseases (Crohn's disease, tumors, cancers...).

2.2. Wearable Antennas

They are used in measurement and data transfer applications of gadgets worn on or near the body (arm, neck, clothing...). Wearable antennas can be used as an interface between implantable or endoscopic antennas and external receivers. They can also directly transmit data collected by the equipment which is an integral part of other sensors.

Due to their proximity to the body, the performance of the antenna is impaired, so the use of suitable antennas is essential. Artificial Magnetic Conductors (AMC) antennas can be used in the one proposed by Agarwal K, Guo Y and Salam B in [4], where the authors used a double layer of AMC material to increase the radiation efficiency of a Yagi antenna to 78.97% and reduce its SAR to 0.714 W/Kg.

To minimize the effect of the body on the performance of wearable antennas, metamaterial can also be used. In [5] authors used 2 × 2 metamaterial cells to improve the performance of a U-shaped patch antenna. After placement of the metamaterial cells the gain of the antenna reached 7.5 dBi and the relative bandwidth was 14.5%. The weakness of this antenna is the complexity of the structure for mass production.

2.3. Implantable Antennas

An implant is a device placed in a body tissue other than a cavity for the purpose of collecting and monitoring key physiological data from a patient and sending it to a remote node on or off the body. The most well-known implants today are intraocular implants, cardiac defibrillators (ICDs), neural brain monitoring implants, and Electromyogram (EMG) implants [6]. But increasingly, they are also being used to measure vital parameters in people exposed to major pathologies. Implants must be distinguished from endoscopes that are necessarily placed in cavities as described in the subsection dealing with endoscopy antennas.

2.4. Challenges of Biomedical Telemetry Antennas

Antennas used in biomedical telemetry must comply with many limitations. According to [7], for an implantable antenna, these constrains concern size, resonance frequency, good biocompatibility, good impedance matching. According to [8], in-body antennas must also have omnidirectional radiation to be able to communicate with sensors outside the body. Other criteria are also important, such as the miniaturization criteria of the antennas defined by Harold W [9], the dimensions of the implants or medical capsules, the flexibility of the substrate and the radiating element, the optimization of the power consumption, the adaptation of the bandwidth to the video transmission and above all the relatively low frequency band defined for the Radio medical communications (Med Radio).

Numerous studies have been conducted on the propagation inside the body and the antennas used. It has been found that satisfying one or more of the constraints often degrades the performance of the other specifications. For example, in paper [10], Ala Alemaryeen proposed a miniature of 18 × 10 mm^2 folded shape antenna for implants of various tissue characteristics. Simulated in an 80 × 80 × 80 mm^3 Phantom, for a reflection coefficient of -10 dB, the antenna exhibits good impedance matching (−30 dB) and a bandwidth of 532 MHz. In addition, the maximum gain of the antenna is −28 dBi, which seems very low for efficient long-range transmission. Furthermore, the author does not specify the size of the implant around which the antenna is wrapped, nor the adaptation of the antenna in the presence of electronic components inside the implant. Different frequency bands have been regulated for biomedical transmission. In [2] [10] these bands have been listed according to the following classification:

- Ultra-Wide Band (UWB): 3100 - 10,600 MHz;
- Medical Body Area Network (MBAN): 2360 - 2400 MHz;
- Medical Implant Communication Service (MICS): 402 - 405 MHz;
- Medical Device Radio communications Service (MediRadio): 401 - 406 MHz;
- 413 - 419 MHz, 426 - 432 MHz, 438 - 444 and 451 - 457 MHz;
- Industrial Scientific and Medical (ISM) band: 433.05 - 434.79 MHz; 902 - 928 MHz; 2400 - 2483.5 MHz; 5725 - 5850 MHz;
- WMTS bands: 608 - 614 MHz; 1395 - 1400 MHz; 1427 - 1432 MHz.

Different biocompatible materials are used as substrate or superstrate in the design of antennas radiating into the human body. **Table 1** hereafter illustrates the main substances used. As most of the tissues are dielectric supers, their permeability is very close to that of air. This leads us not to specify this characteristic in this table. Complex permittivity's are measured at frequencies ranging from 100 MHz to 1 GHz, so there is little variation in these values for frequencies near this range.

Most of the materials used are polymers. The radiation of an antenna inside a tissue depends on the characteristics of the tissue. The characteristics vary according to the type (stomach, intestine, muscle…), the age, the gender of the individual and especially the location of the tissue (skull, abdomen, trunk, legs…). The tissues have high permittivity and low conductivity. In the following **Table 2** extracted from the survey [2] we can find the average characteristics of the main tissues.

Table 1. Biocompatible materials used as substrate or superstrate.

Ref.	Materials	ε_r	Tan δ
[11] [12]	LCP1/Kapton	3.5	0.0027
[11]	Alumine (Al2O3)	9.9	0.0001
[13]	PDMS2	2.8	0.005
[14]	Rogers 3010	10.2	0.0035
[15]	Ultem,	3.15	0.0013
[16]	Teflon	2.17	0.05
[12]	Biofila Silk	2.8	0.01
[17]	FR-4	4.7	0.025

[1]Liquid Crystalline Polymer, [2]Poly Di Methyl Siloxane; ε_r and tan δ represent the relative permittivity and loss tangent, respectively.

Table 2. Characteristics of the main tissues of the human body.

Tissues	Relative Permittivity (ε_r)	Conductivity σ (S/m)
Muscles	52.729	1.7380
Stomach	62.158	2.2105
Small intestine	54.125	3.1731
Colon	53.879	2.0383

To design an antenna that will radiate with minimal loss and acceptable gain, it is necessary to know the characteristics of the tissue in which the antenna will be inserted.

There are different methods to miniaturize and adapt biomedical telemetry antennas. The most well-known techniques are among others the winding of the radiating strand, the creation of slots, the insertion of electronic components and the use of metamaterials. In [15], authors proposed a broadband capsular antenna for biotelemetry applications. The antenna with dimensions of 12 × 6 × 0.035 mm3 is an E-shaped meander etched on a capsule of 11 mm diameter and 24 mm length. The biocompatible Ultem substrate used has a relative permittivity of 3.15 and a conductivity of 0.0013 S/m. Implanted in a body, for a return loss limited to −10 dB, the authors obtained a bandwidth of 7.31 GHz and gains of −25.23 dBi in the human model of three layers (80 mm of muscle, 8 mm of fat, 2 mm of skin). The weakness of this antenna lies in the drop of the antenna gain in the presence of electronic components, particularly the battery.

3. Proposed Antennas

3.1. Structure of the Proposed Antenna

Antenna Design Steps

The antenna developed by R. Alrawashdeh *et al.* in [18] inspires the shape of the suggested antenna but its shape has been revised to optimize its operation.

In the 1st step of the design, we unified the width of the radiating strands at 1 mm and replaced the vertical elements with circular arc elements with a diameter of 2 mm. By integrating the circular arcs, we aim to achieve harmonious radiation and lengthen the electron path. In fact, the gradual 180˚ turn of the electrical charges when changing direction eliminates unwanted radiation and lowers the resonant frequency.

In the second phase of antenna design, 4 arcs were symmetrically integrated into the upper and lower horizontal strands. The arcs allow the resonant frequency to drop to a much lower frequency and balance the current distribution.

Figure 1 shows the geometry of the antenna when extended and when wrapped around an implant of 3.5 mm radius and 10 mm height [18].

The length (L) of the lower strand is 20 mm and that of the upper strands (L_1) and (L_2) is 3.37 mm. The diameter (D_1) and (D_2) of the upper arcs is 2.26 mm. The gap (E) between the central arcs has been dimensioned at 1.6 mm and the horizontal sections (S_1), (S_2), (S_3) have common lengths of 2.66 mm. The height (H) of the implant is 10 mm.

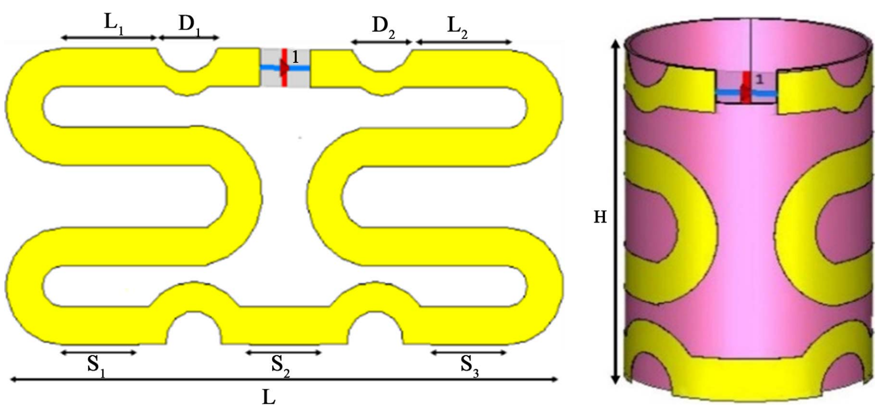

Figure 1. Antenna geometry (a) spread shape (b) shape wrapped around a 3.5 mm radius implant.

3.2. Simulation Results and Discussion

Electromagnetic simulation software was used to perform the simulations. Figure 2 and Figure 3 show the simulation results of the new antenna structure in the muscle characterized by the paper [18]. The muscle has a permittivity and dielectric constant equal to $\varepsilon_{rmuscle} = 57$ and $\sigma = 0.79$ s/m respectively. The dimensions of the human phantom were also kept at $180 \times 100 \times 50$ mm^3. We have chosen the elliptical cylinder shape of the Phantom to better approximate the real shape of most human muscles.

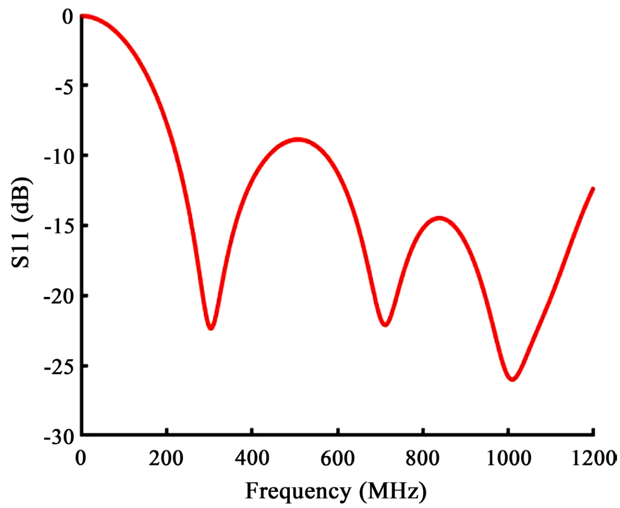

Figure 2. Simulated reflection coefficient (S11) of the antenna.

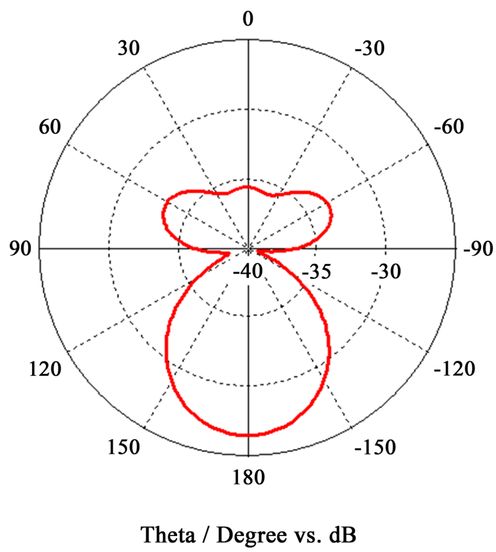

Figure 3. 3D radiation pattern of the meander antenna.

As shown in **Figure 2**, the antenna has two modes of resonance which correspond respectively to bandwidths of 203.7 MHz and 673.7 MHz. The first resonance occurring at the frequency of 304.6 MHz extends from 224.3 MHz to 428 MHz and the second resonance that occurs at the frequency of 1010.8 MHz covers the frequency range from 576.3 MHz to 1200 MHz. The first resonance mode has therefore moved to low frequencies. The integration of the circles has also improved the adaptation. At the first resonance, the simulated reflection coefficient is −22.56 dB and at the second resonance, it is −25.20 dB. **Figure 3** also shows that the maximum gain achieved has increased from −28.4 dBi to −26 dBi. Furthermore, the radiation is mainly in the plane (xoz) orthogonal to the antenna axis. However, it is obvious that neither bandwidth covers the 400 MHz bands (401 –

457 MHz) dedicated to medical communication services.

Table 3. summarizes the comparative study of the performance of the initial antenna with that of the antenna integrating the arcs.

Table 3. Comparison of the radiation characteristics of the right-angle antenna and the antenna with the arcs of a circle.

Characteristics	Antenna with right angles [18]	Antenna integrating arcs of a circle
Bandwidth (MHz)	327 - 530	224 - 428 576.3 - 1200
S11 parameter (dB)	−22	−22.56 −25.2
Maximum gain (dBi)	−28.4	−26

4. Miniaturized Antenna

4.1. Antenna Miniaturization Process

The drop of the first resonance mode to 304.6 MHz after arcs integrating gives the possibility to reduce the dimensions of the antenna.

We wanted to miniaturize the antenna so that once implanted in the body the bandwidth covers all biomedical frequencies up to 1 GHz. The targeted bands constitute 60% of the frequency bands allocated to the transmission of data for biomedical applications. These bands are the most used because of their low propagation losses in the body and the low risk of ionization of human tissue. To achieve this objective, the first resonance mode should be at 500 MHz. By application of the three rules, this theoretically gives a reduction of 40%. At this reduction ratio, two modes of resonance appear respectively at 554.4 MHz and at 1337 MHz but most of the medical bands are not covered. Also, the antenna is almost broadband. To therefore unify the two passbands, we sought by simulation an intermediate resonance frequency between the two resonance frequencies. The simulation proved that at a size of 9.4×4.7 mm^2, the antenna resonates at 562.8 MHz with coverage of all biomedical frequency bands up to 1 GHz. Applying the same rule of three, this corresponds to a theoretical reduction of 45.88%. But if we consider the simulated size of the antenna, it appears that the antenna has been reduced to 47% of its initial size. The area of the reduced antenna is thus reduced from 20×10 m^2 to 9.4×4.7 m^2.

4.2. Miniaturized Antenna Performances

The miniaturized antenna was simulated in the same conditions of the human Phantom as in the paper [18]. Figure 4 and Figure 5 show the simulation results of the S11 and the reduced antenna radiation pattern. The antenna has been reduced by 53% compared to its initial size. The occupied volume of the proposed antenna is 1.122 mm^3 ($9.4 \times 4.7 \times 0.0254$ mm^3).

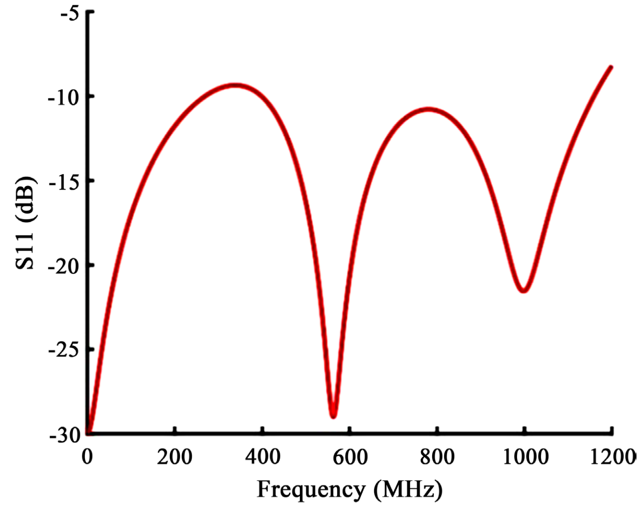

Figure 4. Simulated reflection coefficient (S11).

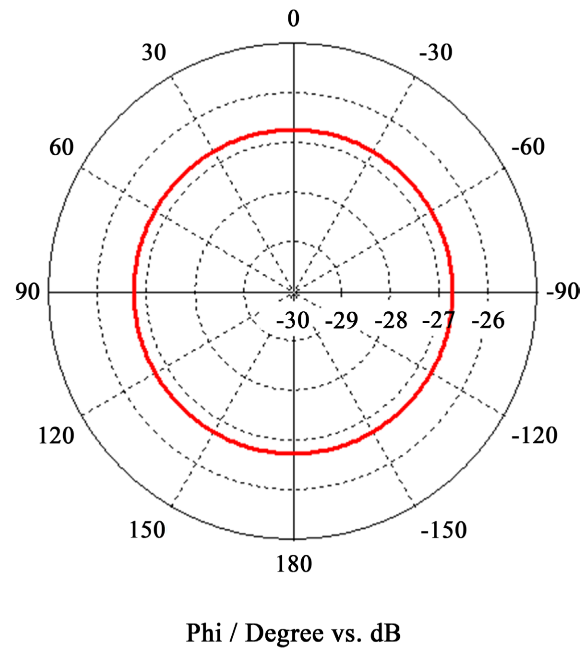

Figure 5. 2D radiation pattern.

Through **Figure 4** and **Figure 5**, with the reduction, the antenna remains dual band but each of these bands has been widened. The first band, which covers the range from 10 Hz to 270 MHz has a bandwidth of 270 MHz. This band can be used in the downlink transmission of biomedical communication systems [19] for the administration of products or the activation of a patient treatment process. The second bandwidth extending from 397.2 MHZ to 1159.2 MHZ is 762 MHz wide. This mode covers the MIC (402 - 405 MHz), MediRadio (401 - 457 MHz), ISM (902 - 928 MHz) and WMTS (608 - 614 MHz) bands which are regulated for the transmission of uplink data in biomedical communication systems. The antenna can be used in implantable connected objects to communicate with long-range IoT gateways (LoRa, Sigfox) that are currently transmitted in the 868 MHz band (ISM868).

The matching and maximum realized gain of the antenna have also improved. Table 4 shows the simulated performance of the reduced antenna.

Table 4. Comparison of the radiation characteristics of the miniaturized antenna and the structures with right angles and arcs.

Characteristics	Antenna with right angles [18]	Antenna integrating the arcs of a circle	Miniaturized antenna
Bandwidth (MHz)	203	204 623.7	270 762
S11 Parameter (dB)	−22	−22.56 −25.2	−30 −29.09
Maximum gain realized (dBi)	−28.4	−25.1	−26.7

4.3. Effects of the Internal Electrical Components of the Implant

Inside the implants are assembled small electronic equipment providing useful functions. That equipment, which is mostly made of conductive materials, can affect the performance of the antenna. The most unpleasant of these devices is the battery. It can act as an unidimensional ground plane whose effect on the matching will be unpredictable. It can also generate a static electric field, which can alter the radiation pattern of the antenna. To study the effect of internal components, we modeled the battery by a perfect cylindrical conductor (PEC) of 5 mm diameter and 10 mm height. We varied the distance (d) between the antenna and the battery by varying the diameter of the battery.

Figure 6 shows a modelled battery inside an implant and Figure 7 shows the variations of the simulated reflection coefficient for different distances.

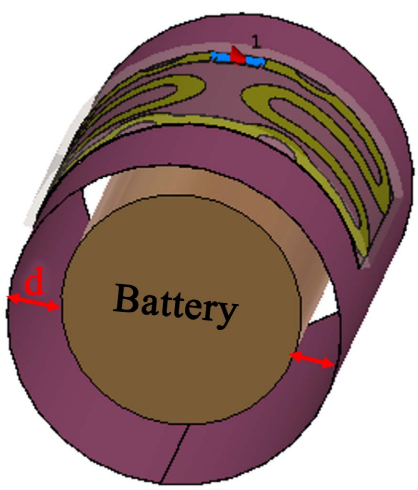

Figure 6. Modelled battery inside an implant.

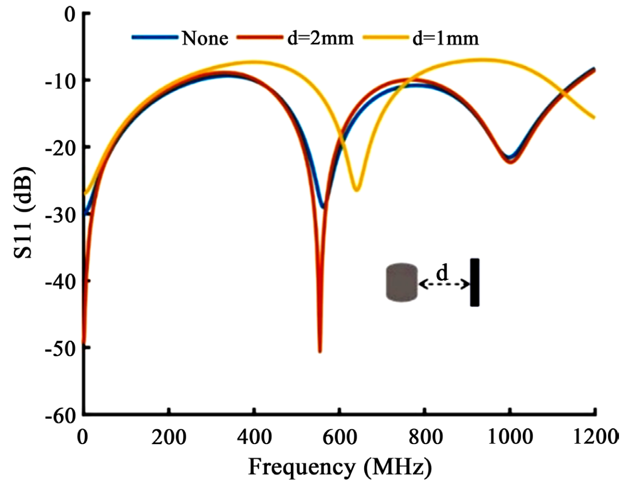

Figure 7. S11 simulated in presence of battery.

The analysis of this curve shows (see **Figure 7**) that when the battery is moved away from the antenna, the antenna matching improves reaching −50.57 dB for a distance d of 2 mm. However, as the battery gets closer to the antenna, its matching degrades, and the resonance shifts to higher frequencies. However, the antenna retains its performance in the presence of internal electronic components with a distance (d) more than 1mm.

4.4. Effect of Permittivity and Conductivity Variation

Since the characteristics (permittivity, conductivity) of human body can vary according to organ, gender, and age, we wanted to analyze the effect of any variation of these quantities on antenna performance. We therefore varied relative permittivity from 54 to 60 and conductivity from 0.59 S/m to 1.09 S/m. These values are those that a muscle can assume, depending on age and part of the body, at frequencies above 1 G Hz.

Figures 8(a) and **Figures 8(b)** illustrate the variation curves of the reflection coefficient for these different permittivity and conductivity values.

For relative permittivity below 56, the S11 parameters of the first resonance mode and the resonance frequency of the second resonance mode drop, respectively.

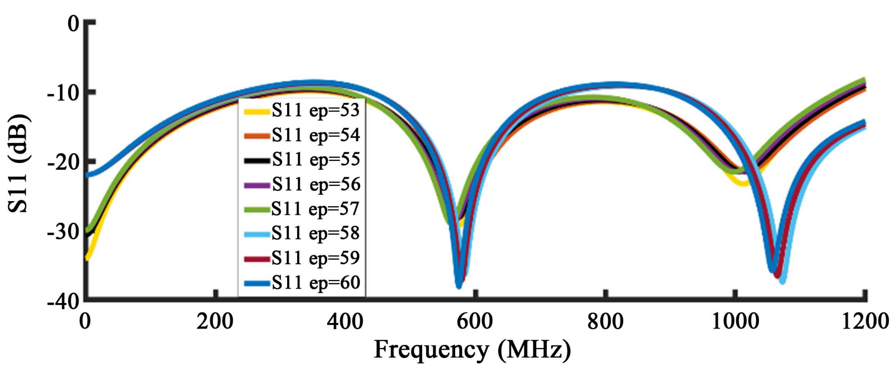

(a)

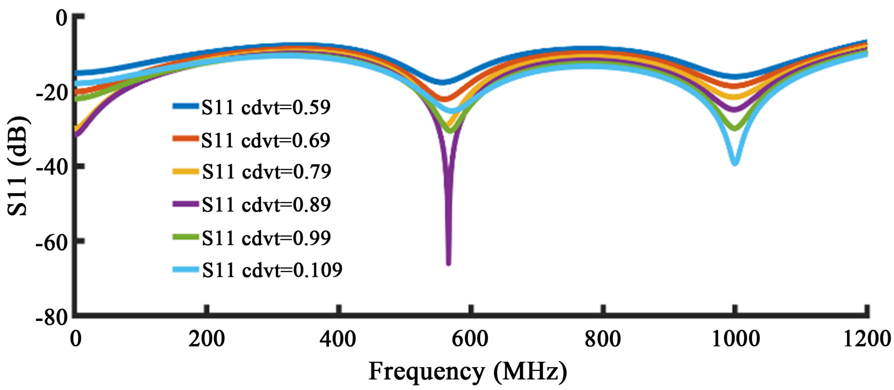

(b)

Figure 8. Simulated S11 variation (a) according to the relative permittivity, (b) according to the conductivity.

But for relative permittivity values above 56, the reflection coefficient remains unchanged. Moreover, despite the change in permittivity, the reflection coefficient remains below −10 dB overall. Analysis of the curve in **Figures 8(a)** shows that, although the conductivity of the body varies, the reflection coefficient remains below −10 dB, and the two resonance modes retain their same resonance frequencies. These two simulations prove that the antenna can be used in different parts of the body while maintaining the same performance.

4.5. Comparison of the Results with Those Existing in Literature

In **Table 5**, we compared the antenna performances with those of antennas listed in the literature. The proposed antenna dimensions (44.18 mm^2) appear to be the smallest but it performs better than the other antennas. It covers 5 bands (402, 433, 614, 868, 915 MHz) including the 868MHz band which is currently successful in IoT connectivity. This band could be used to popularize the IoMT (Internet of Medical things). Moreover, the size of the antenna allows it to be implanted in small muscles such as those of the fingers. The antenna also radiates in the 160 MHz band used for downlinking between outdoor transmitters and implants.

5. The Specific Absorption Rate (SAR)

Tissue ionization is one of the most feared hazards by implant wearers. To remove this ambiguity, we wanted to check the Specific Absorption Rate (SAR) related to the use of the proposed antenna. According to [20], the SAR values of implantable antennas should be between 1.6 W/Kg per 1 g of tissue and 2 W/Kg per 10 g of tissue to prevent dangerous tissue heating.

We considered the frequency 401 MHz of the MedRadio band to evaluate the SAR. According to the article [20], the SAR can be calculated by using the equation (1).

$$\text{SAR} = \frac{P}{\rho} = \frac{\sigma|E|^2}{2\rho} \quad (1)$$

P is the power density losses (W/m^3), ρ and σ are the density (Kg/m^3) and conductivity (S/m) of the tissue, E is the electric field ($\vec{E}$) generated. To determine P, we related the PL power lost in the tissue to the volume (V) of the Phantom under consideration. This allows us to rewrite the SAR expression with equation (2).

$$\mathrm{SAR} = \frac{P_L}{\rho V} \quad (2)$$

To feed the antenna excitation port during the simulation, a Gaussian voltage with a maximum value of 1 volt was produced. This voltage allowed to radiate a power of 0.03 mW for a power of 450.80 mW received (accepted). The power (PL) absorbed by the tissue is so 450.77 mW. The density of the muscle at that frequency is 1041 Kg/m^3 and the conductivity is 0.79 S/m. The calculated SAR value is therefore 0.48 W/Kg. This value is quite low compared to the references given by ICNIRP (International Commission on Non-Ionizing Radiation Protection) but the EIRP (Effective, Isotopically Radiated Power) of −15.23 dBm is slightly higher than −16 dBm defined as the maximum EIRP for implants. Therefore, to use the proposed antenna without damage, an excitation voltage of less than 1 V is required to feed.

Table 5. Comparative table of antenna performance with other antennas.

References	Frequences (MHz)	Volumes (mm^3)	Bandwidths (MHz)	Maximum realized gains (dBi)	Antenna structures	Antenna dimensions (mm^2)	Phantom: tissue, size, implantation depth (mm^3)
[18]	402 433	5.08	203	−28.4	Meander	20 × 10	180 × 100 × 50
[21]	401	193.2	50	−19.99	Monopole antenna	28 × 11.5	180 × 60 × 60
[22]	2.45	9.8	483	−12	Circular shaped	7 × 7	50 × 50 × 50
[10]	433	6.3	532	−28.5	E-sharp	18 × 10	80 × 80 × 80
[23]	915	12.446	230	−28	bear-shaped	7 × 7	25 × 25 × 25
Proposed antenna	402 433 614 868 915	1.10	270 762	−26.7	Meander	9.4 × 4.7	180 × 100 × 50

6. Conclusions

In this paper, a meander antenna for biomedical implant applications has been proposed. Compared to its initial geometry, the antenna integrates circular arcs that control its operation. The integration of the arcs allowed us to miniaturize the antenna to a volume of 1.122 mm^3 and to improve the performance. The performances reached both in terms of bandwidth (762 MHz), matching (−30 dB), gain (−26.7 dBi) and especially in terms of size (9.4 × 4.7 mm^2) making this antenna a potential candidate for implantable sensors.

Moreover, we are working on making the antenna reconfigurable and improving its gain so that it can be proposed for other applications.

Acknowledgements

The authors would like to thank the Research and Technological Innovation Department of the Ecole Supérieure Africaine des Technologies de l'Information et de la Communication (ESATIC).

Conflicts of Interest

The authors declare no conflicts of interest regarding the publication of this paper.

References

[1] Caterina, Hayat and Guillorel (2011) Study on Information Technologies in the Service of New Care Organizations, Study Report. OPIIEC. https://www.syntec-ingenierie.fr/wp-content/uploads/2019/06/2011-06-01.Etude-OPIIEC.telemedecine.pdf

[2] Gupta, A., Kansal, A. and Chawla, P. (2021) A Survey and Classification on Applications of Antenna in Health Care Domain: Data Transmission, Diagnosis and Treatment. *Sādhanā*, **46**, Article No. 68. https://doi.org/10.1007/s12046-021-01586-4

[3] Izdebski, P.M., Rajagopalan, H. and Rahmat-Samii, Y. (2009) Conformal Ingestible Capsule Antenna: A Novel Chandelier Meandered Design. *IEEE Transactions on Antennas and Propagation*, **57**, 900-909. https://doi.org/10.1109/tap.2009.2014598

[4] Agarwal, K., Guo, Y. and Salam, B. (2016) Wearable AMC Backed Near-Endfire Antenna for On-Body Communications on Latex Substrate. *IEEE Transactions on Components, Packaging and Manufacturing Technology*, **6**, 346-358. https://doi.org/10.1109/tcpmt.2016.2521487

[5] Ashyap, A.Y.I., Zainal Abidin, Z., Dahlan, S.H., Majid, H.A. and Saleh, G. (2018) Metamaterial Inspired Fabric Antenna for Wearable Applications. *International Journal of RF and Microwave Computer-Aided Engineering*, **29**, e21640. https://doi.org/10.1002/mmce.21640

[6] Garcia-Pardo, C., *et al.* (2018) UWB Propagation Environment for Medical In-Body Sensor Networks. *IEEE Antennas and Propagation Magazine*, **60**, 19-33.

[7] Wu, Q.-H., *et al.* (2020) A Miniaturized Implantable Planar Inverted-F Antenna for Bio-Telemetry Applications at 2.45 GHz Industrial, Scientific, and Medical Band. *Microwave and Optical Technology Letters*, **62**, 391-396.

[8] Garcia-Pardo, C., *et al.* (2018) Ultrawideband Technology for Medical In-Body Sensor Networks: An Overview of the Human Body as a Propagation Medium, Phantoms, and Approaches for Propagation Analysis. *IEEE Antennas & Propagation Magazine*, **60**, 19-33.

[9] Wheeler, H.A. (1947) Fundamental Limitations of Small Antennas. *Proceedings of the IRE*, **35**, 1479-1484. https://doi.org/10.1109/jrproc.1947.226199

[10] Alemaryeen, A. (2021) On the Sensitivity of Implantable Antenna Performance to Variations in the Electrical Properties of Body Tissues. 2021 *International Symposium on Networks, Computers and Communications* (*ISNCC*), Dubai, 31 October-2

November 2021, 1-4. https://doi.org/10.1109/isncc52172.2021.9615654

[11] Nikolayev, D. (2017) In-Body Antenna for Miniature Biotelemetry Capsules: Increasing Robustness and Radiation Efficiency. URSI-France Journées Scientifiques 1/3 Février. https://univ-rennes.hal.science/hal-01561084

[12] Alemaryeen, A. (2021) Compact Wideband Antenna for Wireless Capsule Endoscopy System. *Applied Physics A*, **127**, Article No. 271. https://doi.org/10.1007/s00339-021-04420-0

[13] Loktongbam, P. and Solanki, L.S. (2017) Design and Analysis of an Implantable Patch Antenna for Biomedical Applications. *International Journal of Engineering Technology Science and Research* (*IJETSR*), **4**, 126-138.

[14] Hasan, R.R., *et al*. (2019) In Body Antenna for Monitoring Pacemaker, International Conference on Automation, Computational and Technology Management (ICACTM). Amity University.

[15] Alemaryeen, A., *et al*. (2019) A Wideband Antenna for Biotelemetry Applications: Design and Transmission Link Evaluation. *Applied Computational Electromagnetics Society Journal*, **33**, 1129-1130.

[16] Baek, J.J., Kim, S.W. and Kim, Y.T. (2019) Camera-Integrable Wide-Bandwidth Antenna for Capsule Endoscope. *Sensors*, **20**, Article No. 232. https://doi.org/10.3390/s20010232

[17] Sulaiman, N.H., Samsuri, N.A., Rahim, M.K.A., Inam, M. and Seman, F.C. (2018) Low Profile Compact Meander Line Antenna for Pacemaker Applications in MICS Band. 2018 *IEEE Asia-Pacific Conference on Antennas and Propagation* (*APCAP*), Auckland, 5-8 August 2018, 1-2. https://doi.org/10.1109/apcap.2018.8538229

[18] Alrawashdeh, R., Huang, Y. and Cao, P. (2013) Flexible Meandered Loop Antenna for Implants in Medradio and ISM Bands. *Electronics Letters*, **49**, 1515-1517. https://doi.org/10.1049/el.2013.3035

[19] PillCamTM. Capsule Endoscopy Order Information. https://www.medtronic.com/covidien/en-us/products/capsules-endoscopy/pillcam-crohns-system.html

[20] Alrawashdeh, R., Huang, Y. and Abu Bakar Sajak, A. (2014) A Flexible Loop Antenna for Biomedical Bone Implants. *The* 8*th European Conference on Antennas and Propagation* (*EuCAP* 2014), The Hague, 6-11 April 2014, 861-864. https://doi.org/10.1109/eucap.2014.6901898

[21] Nguyen, V.T. and Jung, C.W. (2016) Radiation-Pattern Reconfigurable Antenna for Medical Implants in Medradio Band. *IEEE Antennas and Wireless Propagation Letters*, **15**, 106-109. https://doi.org/10.1109/lawp.2015.2432172

[22] Bashir, Z., Zahid, M., Abbas, N., Yousaf, M., Shoaib, S., Asghar, M.A., *et al*. (2019) A Miniaturized Wide Band Implantable Antenna for Biomedical Application. 2019 *UK*/*China Emerging Technologies* (*UCET*), Glasgow, 21-22 August 2019, 1-4. https://doi.org/10.1109/ucet.2019.8881849

[23] Ahmad, S., Manzoor, B., Paracha, K.N., Haider, S., Liaqat, M., Al-Gburi, A.J.A., *et al*. (2022) A Wideband Bear-Shaped Compact Size Implantable Antenna for In-Body Communications. *Applied Sciences*, **12**, Article No. 2859. https://doi.org/10.3390/app12062859